

A Facile Route for Preparation of High-Performance Hierarchical Porous Carbons for Supercapacitor Electrodes

Lili Wang^{*}, Miaomiao Jia, Wenqi Lu, Kunlong Yang, Junqin Fan, Gang Liao, Jianguo Yu^{*}

College of Environment and Chemical Engineering & State Key Laboratory of Hollow-Fiber Membrane Materials and Membrane Processes, Tianjin Polytechnic University, Tianjin 300387, PR China
College

^{*}E-mail: wanglili09.29@163.com, hh_y1118@hotmail.com

Received: 31 March 2016 / Accepted: 7 April 2016 / Published: 4 June 2016

In this work, a facile route for preparation of high-performance hierarchical porous carbons from starch was described. The hierarchical porous carbons with developed micropores and mesopores were prepared, and the pore size was distributed at 2, 9 and 13 nm. The high-performance porous carbons with specific capacity of 221 F/g was obtained when the mass ratio of starch to zinc nitrate was 1:1 and the carbonization temperature was 800 °C. It also possessed excellent specific capacitance retention about 96.4 % of the initial value even after 5000 cycles, and the higher capacitance retention of 88.7% was obtained when the current density changing from 0.2 to 2 A/g. The pore structure and the electrochemical performance could be tuned by changing the reaction conditions. The experimental results suggested the hierarchical porous carbons could be an ideal candidate for supercapacitor applications.

Keywords: Starch, Hierarchical porous carbons, Supercapacitor, Specific capacity

1. INTRODUCTION

Recently, supercapacitors have become an important energy storage system owing to their high energy density, power density and long cycle stability compared to batteries [1-4]. It is great interested in developing high performance supercapacitors due to the urgent needs in the field of electronics, heavy electric vehicles, and industrial power management [5-7]. Carbons materials, transition metal oxides and electronically conducting polymers are under close scrutiny for used as supercapacitor electrode materials [8-12], which greatly influenced the capacitance performance of supercapacitors. Among various electrode materials, porous carbons are considered to be a promising candidate for application in supercapacitors due to the lowcost, high surface area, high chemical stability and better

electronic conductivity [13-17]. So, it is significant to controllably prepare porous carbon materials with graded micro- and mesoporous structures. The commonly preparation methods include template method [18-21], carbonization of polymer [22], physical activation and chemical activation [23-26]. The templates like familiar inorganic zeolite and silica could be generally used to prepare porous carbon with tailored pore sizes and textures [21]. However, it is hard to prepare hierarchical porous carbons with wide pore size distribution using the uniform structure of templates. Therefore, it is necessary to investigate the preparation of higher-performance porous carbons with wide pore size distribution by a facile route.

In this work, the hierarchical porous carbons with wide pore size distribution were prepared from starch. Zinc oxide derived from the thermal decomposition of zinc hydroxide in the carbonization process of pretreated starch was the template. The obtained hierarchical porous carbons had developed micropores and mesopores. The effects of reaction conditions such as the mass ratio of starch to zinc nitrate and carbonization temperatures on the specific surface area, pore volume, and pore size distribution of porous carbons have been studied. Moreover, the electrochemical property of obtained porous carbons was investigated in detail, which indicated the products could be an ideal candidate for supercapacitor applications.

2. MATERIALS AND METHODS

2.1. Materials

Starch was obtained from Shandong Jincheng Co., Ltd. Zinc nitrate, urea, potassium hydroxide, acetylene black, poly tetrafluoroethylene and hydrochloric acid used in this work were of analytical grade, and they were purchased from Beijing Chemicals Co. Ltd. Distilled water was applied in all the processes of synthesis and treatment.

2.2. Preparation of hierarchical porous carbons

Typically, 7.0 g starch, 3.5 g (7.0 g, 14.0 g) ZnNO_3 (the mass ratio of starch to ZnNO_3 was 2:1, 1:1 and 1:2, respectively) and 60 ml deionized water were successively loaded into a 500 ml three-neck round-bottom flask equipped with a thermometer and a mechanical stirrer, the mixtures were heated to 100 °C for a certain time until starch was gelatinized, then 0.7 g urea was added into the mixtures, and the mixtures were constantly stirred at 150 °C for 5 hours, then the mixtures were placed into an oven with designed temperature of 80 °C for a certain time until the weight of mixtures was constant, which was the precursor of hierarchical porous carbons. The carbons precursor was carbonized in a tube furnace at 700, 800 and 900 °C for 2 hours with a heating rate of 3 °C/min under N_2 atmosphere, respectively. Finally, the ZnO/C composite materials were obtained. The composite materials were washed with HCl of 2 mol/L and distilled water until pH = 7, then the hierarchical porous carbons were dried in an oven at 120 °C overnight and the final products were obtained .

2.3. Analysis

Characterization of the hierarchical porous carbons were carried out by nitrogen adsorption-desorption isotherms, which were measured at 77 K using Micromeritics instrument (ASAP 2020). Before the measurement of gas adsorption, the porous carbons were degassed at 300 °C under vacuum for 3 h. The BET surface area were calculated from N₂ adsorption isotherms by the equation of Brunauer-Emmett-Teller (BET). The total pore volumes were estimated when the relative pressure was 0.995.

The structure and composition of the hierarchical porous carbons were analyzed by X-ray powder diffraction (SHIMADZU XRD-6000 diffractometer with Ni-filtered Cu K α radiation, the scanning rate was 10°/min and 2 θ was ranged from 10 to 80°).

The morphology and size of the hierarchical porous carbons were examined using a Hitachi H-800 transmission electron microscope (TEM), at an accelerator voltage of 200 kV.

The surface property of the samples was quantitatively analyzed by X-ray photoelectron spectroscopy (XPS, Thermo ESCALAB 250).

The electrochemical performance of the hierarchical porous carbons were carried out in three electrode configuration in 6 mol/L KOH aqueous solution. The working electrode was fabricated as follows: 80 wt.% porous carbon, 10 wt.% acetylene black and 10 wt.% poly (tetrafluoroethylene) was mixed, then the mixture was spread onto a piece of foam nickel (1 cm \times 1 cm), and then they were pressed at 10 MPa. A platinum foil and a saturated calomel electrode (SCE) were used as the counter electrode and the reference electrode, respectively. All the electrochemical measurements were carried on a CHI 660D electrochemical workstation. The cyclic voltammetry (CV) measurement was carried out at the scan rate of 60 mV/s when the potential was ranged from 0 to 1.0 V, and the galvanostatic charge/discharge measurements were performed at the current density of 0.20 ~ 2.0 A/g.

3. RESULTS AND DISCUSSION

Zinc hydroxide was produced from the reaction of zinc nitrate and urea in heating process of starch at 150 °C, and then zinc oxide was generated by the thermal decomposition of zinc hydroxide in carbonization process, therefore, ZnO/C composite materials were prepared. The composite materials obtained at carbonization temperature of 700 °C with the mass ratio of starch to ZnNO₃ of 2:1, 1:1 and 1:2 were defined as ZnO/C-2:1, ZnO/C-1:1 and ZnO/C-1:2, respectively. The corresponding hierarchical porous carbons were obtained when the composite materials were washed with HCl of 2 mol/L and distilled water until pH = 7, which were defined as C-2:1, C-1:1 and C-1:2, respectively. ZnO/C composite materials obtained with the mass ratio of ZnNO₃ to starch of 1:1 at carbonization temperature of 700, 800 and 900 °C were defined as ZnO/C-700, ZnO/C-800 and ZnO/C-900, respectively. The corresponding hierarchical porous carbons were defined as C-700, C-800, C-900, respectively.

3.1. TEM images of ZnO/C composite materials and hierarchical porous carbons

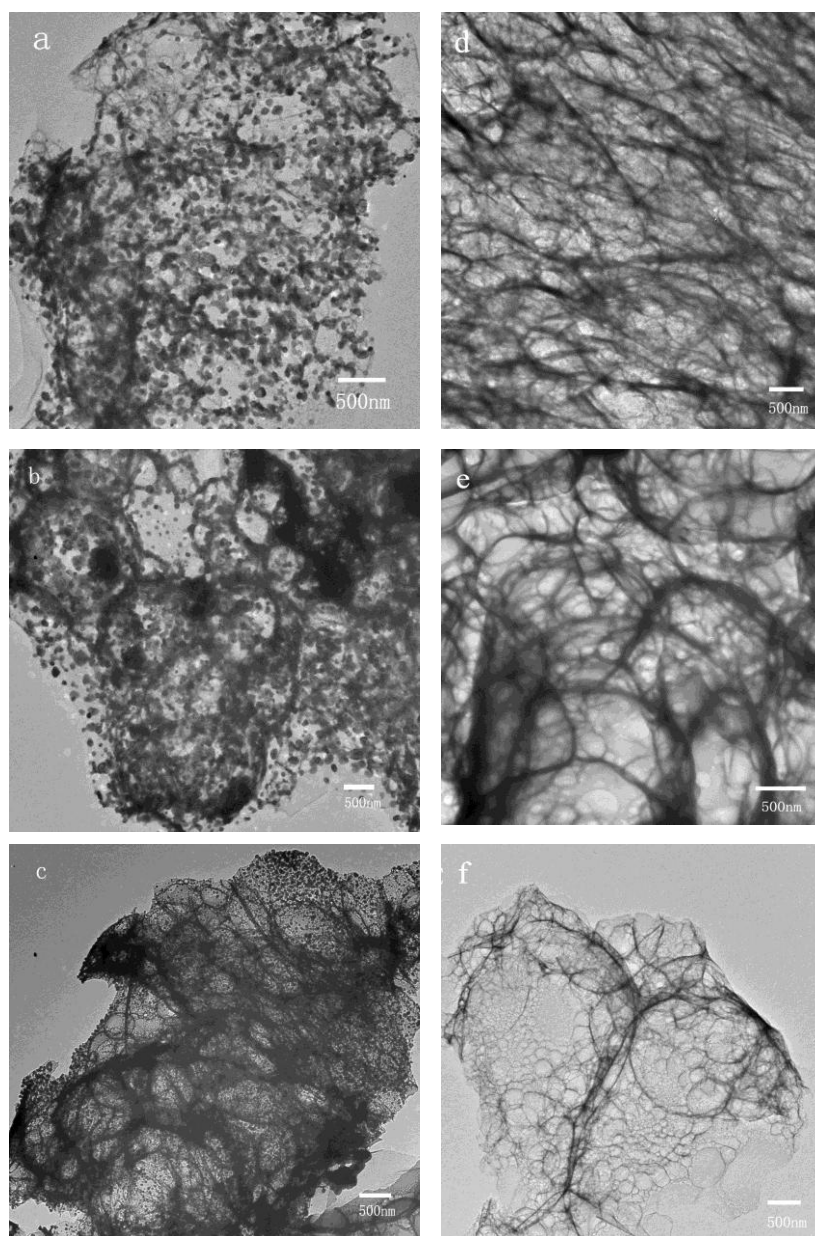


Figure 1. TEM images of (a) ZnO/C-2:1, (b) ZnO/C-1:1, (c) ZnO/C-1:2 and (d) C-2:1, (e) C-1:1 and (f) C-1:2.

Fig. 1 shows the TEM images of ZnO/C composite materials (a, b, c) and hierarchical porous carbons (d, e, f) prepared at carbonization temperature of 700 °C with the mass ratio of ZnNO₃ to starch of 2:1, 1:1 and 1:2, respectively. It can be seen from Fig. 1 (a, b, c) that there were some particles in the carbon materials, which were ZnO nanoparticles derived from the thermal decomposition of Zn(OH)₂. The number and size of ZnO particles were increased with the quality of ZnNO₃ increasing. Fig. 1a shows the particle size of ZnO is relatively large, and they disperses unevenly in the carbon materials. So the pore size of corresponding porous carbons shown in Fig. 1d is larger and the number of pore is relatively less than other porous carbons. ZnO particles were

aggregated due to the excess added of ZnNO_3 , which was not conducive to the formation of pores in carbon materials. Fig. 1b shows that ZnO particles disperses uniformly and the particle size is relatively small. So the corresponding porous carbons contain more crosslinked pores, which facilitate the infiltration of solution and electronic transmission. When the mass ratio of ZnNO_3 to starch is 1:2, the size of ZnO particles is small shown in Fig. 1c, and the crosslinked pores of corresponding porous carbons are less shown in Fig. 1f. The results indicated that the optimum mass ratio of starch to ZnNO_3 was 1:1, which was facilitated to the formation of micropores and mesopores, and it made the porous carbon have good electrochemical performance.

3.2. XRD of ZnO/C composite materials and hierarchical porous carbons

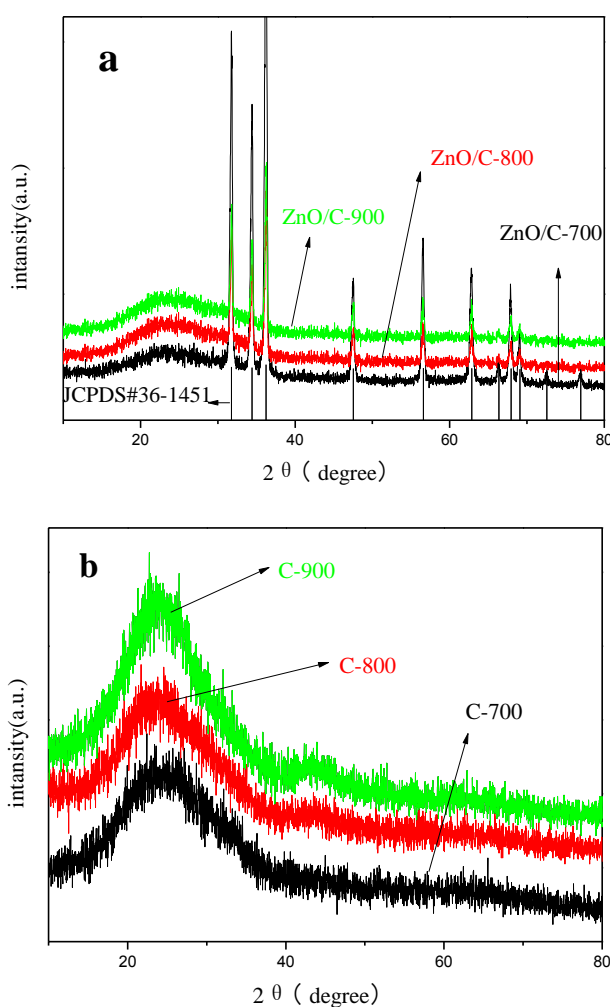


Figure 2. XRD of (a) ZnO/C-700, ZnO/C-800 and ZnO/C-900; (b) C-700, C-800 and C-900.

X-ray diffraction patterns were used to characterize the crystal structures of ZnO/C composite materials and hierarchical porous carbons. Fig. 2(a) presents the XRD patterns of ZnO/C composite materials obtained at different carbonization temperatures (700, 800 and 900 °C), the sharp diffraction peaks at $2\theta=31.77^\circ$, 34.42° , 36.25° , 47.54° , 56.60° , 62.86° , 66.37° , 67.96° , 69.09° , 72.56° and 76.95°

can be attributable to the crystal structures of ZnO. The existence of ZnO was proved by X-ray diffraction and TEM images. The X-ray diffraction patterns shows broad diffraction peaks $2\theta=24^\circ$, which were the incomplete graphitization peaks of carbon.

Fig. 2b presents the XRD patterns of hierarchical porous carbons obtained at different carbonization temperature (700, 800 and 900 °C). The pattern shows a broad diffraction peaks at $2\theta=24^\circ$, which is assigned to the plane of graphite (002), it indicates the existence of graphite crystallites. When the carbonization temperature was higher (800 and 900 °C), the weak diffraction peaks appeared at $2\theta=44^\circ$, which was assigned to the plane of graphite (100). It illustrated higher temperature was beneficial to the formation of localized graphitization. Whereas the carbon material was impossible to completely graphitize in such a lower temperature, so the macroscopy of the samples show amorphous structure. The samples of C-2:1, C-1:1 and C-1:2 had the same structure as the products prepared at different carbonization temperature (C-700, C-800 and C-900).

3.3. N_2 adsorption isotherms and pore size distribution of hierarchical porous carbons

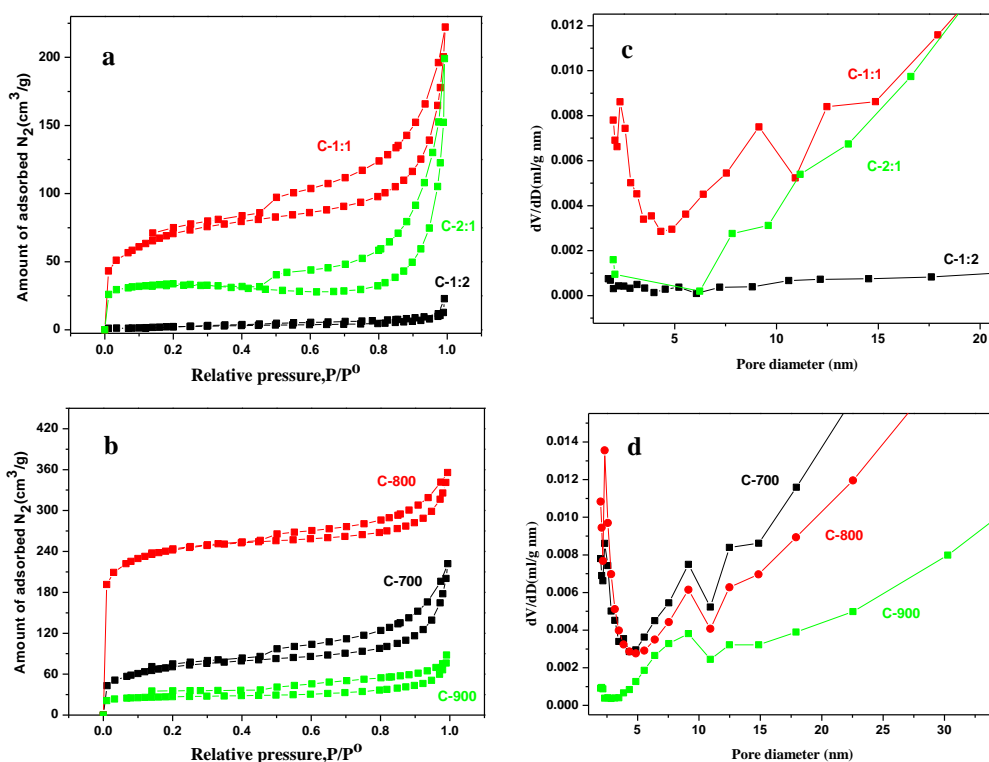


Figure 3. N_2 adsorption isotherms (a, b) and pore size distribution curves (c, d) of hierarchical porous carbons.

N_2 adsorption isotherms and the pore size distribution calculated from adsorption isotherms by the Barrett–Joyner–Halenda (BJH) method of porous carbons are exhibited in Fig. 3. According to the BDDT (Brunauer–Deming–Deming–Teller) classification [23, 24], all the isotherms expect for C-1:2 in this work were classified into type I and IV. It clearly demonstrated that the amount of adsorbed N_2

was increased at the relative pressures lower than 0.1, and there was obvious hysteresis loop at a middle pressure of $P/P^0 = 0.4$, which suggested the presence of capillary condensation. The results indicated there were micropores and mesopores in these products. Fig. 3c shows the pore size distribution, it illustrates that pore size is mainly distributed at 2 nm (microporous) and 8~15 nm (mesoporous), which is in accordance with N_2 adsorption isotherms of the products. The N_2 adsorption isotherm of C-1:2 was classified into type IV, and there was a small hysteresis loop at middle pressure, it indicated that the porous carbons had mesopores and there was nearly no micropores. The less quality of $ZnNO_3$ added in the prepared process was not conducive to the formation of pores in carbon materials. Therefore, there were little pores in the product of C-1:2, which was in accordance with N_2 adsorption and pore size distribution isotherms of the product. The pore structure of porous carbon (C-1:1) was well-developed than other porous carbon, the pore size is mainly distributed at 2 nm (microporous), 9 and 13 nm (mesoporous), it indicated the optimum mass ratio of starch to $ZnNO_3$ was 1:1.

The amount of adsorbed N_2 was not increase sharply when the relative pressures was lower than 0.1, but the hysteresis loop was obvious at $P/P^0 = 0.4$ for C-900, it demonstrated that there were more mesopores than micropores in the products. The pore size distribution shown in Fig. 3d illustrates that pore size is mainly distributed at 2 nm (microporous), 9 and 13 nm (mesoporous), which is in accordance with N_2 adsorption isotherm shown in Fig. 3c. The porous carbon prepared at different carbonization temperatures (700, 800 and 900 °C) with the mass ratio of $ZnNO_3$ to starch of 1:1 had developed mesopores, which facilitated the transmission of electrolyte ions, and it enable the porous carbon have good electrochemical performance.

The Brunauer–Emmett–Teller (BET) surface area (S_{BET}), micropore and mesopore volume (V_{micro} and V_{meso}) of the prepared porous carbons are shown in Table 1.

Table 1. The porous texture characterizations of hierarchical porous carbons.

Samples	S_{BET} (m^2/g)	V_{micro} (cm^3/g)	V_{meso} (cm^3/g)
C-700	236	0.07	0.26
C-800	751	0.26	0.29
C-900	143	0.03	0.20
C-1:2	31	-	0.03
C-1:1	236	0.07	0.26
C-2:1	99	0.06	0.21

The specific surface area of C-800 °C is 751 m^2/g , which is relatively larger than that of other hierarchical porous carbons, and it have more developed pore structure. It indicated that the optimum carbonization temperature was 800 °C and the optimum mass ratio of $ZnNO_3$ to starch was 1:1. Higher temperature would lead to the collapse of pores, so the pore volume and BET surface area of C-900 °C was quite small. Whereas, the pore structure was not sufficiently formed at lower temperature (700 °C). The porous characteristics also influenced by the mass ratio of $ZnNO_3$ to starch, more or less

quality of ZnNO_3 added in prepared process were not good for the formation of pores, so the optimum mass ratio was 1:1.

3.4. XPS spectrum of the C-800 sample

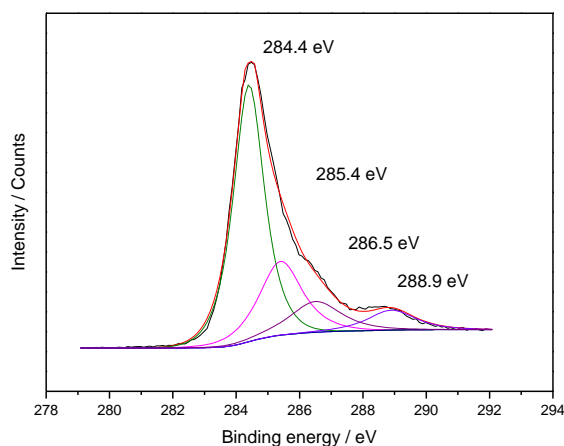


Figure 4. High-resolution C1s XPS of the C-800 sample.

Fig. 4 shows the high-resolution XPS spectrum of C1s peak of C-800 sample. The spectra of C1s peak can be deconvoluted into four components with the binding energy at 284.4, 285.4, 286.5 and 288.9 eV, respectively, and the results are summarized in Table 2.

Table 2. Deconvolution results of XPS spectra of the C1s.

Position (eV)	Assignment	Percentage (%)
284.4	graphite	58.23
285.4	R-OH + C-O-C	23.31
286.5	C=O + >C=O	11.53
288.9	COOH + -C(O) -O-C	6.93

The carbon species correspond to graphite carbon (284.4 eV), carbon in alcohol and ether groups (285.4 eV), carbon in carbonyl groups (286.5 eV) and carboxyl and/or ester groups (288.9 eV) [27]. The percentage of carbonyl groups, carboxyl and/or ester groups was 11.53 and 6.93%, respectively, and the presence of these functional group enabled the sample have good electrochemical performance.

3.5. Electrochemical performances of hierarchical porous carbons

In order to examine the electrochemical performances of obtained hierarchical porous carbons prepared at different carbonization temperature (700, 800 and 900 °C) with the mass ratio of ZnNO_3 to

starch of 1:1, the cyclic voltammetry (CV) and galvanostatic charge discharge measurements were carried out. The specific capacitance of the porous carbons was calculated from the galvanostatic charge-discharge curve using the equation: $C = \frac{i\Delta t}{\Delta V m}$, where C is the specific capacitance obtained from the discharge cycle under constant current charge/discharge measurements, i is the constant current, Δt is the discharge time, ΔV is the potential range, and m is the mass of the sample.

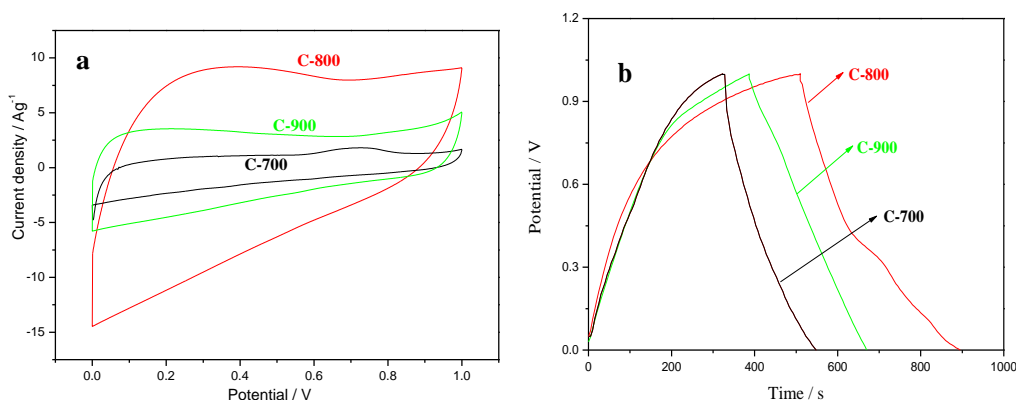


Figure 5. (a) CV curves at the scan rate of 60 mV/s and (b) Galvanostatic charge-discharge curves at the current density of 0.2 A/g of the porous carbons.

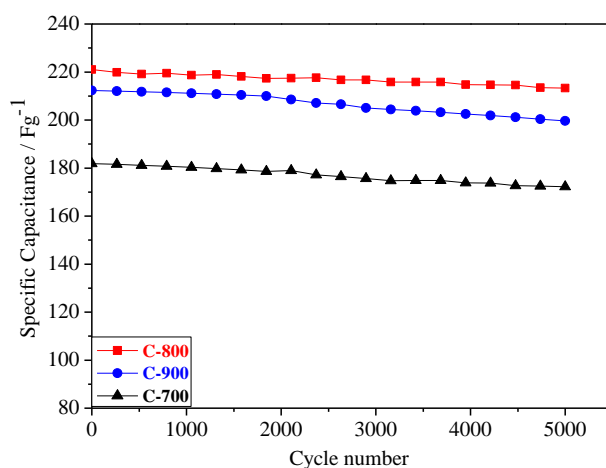


Figure 6. Cycling performance of the porous carbons at a current density of 0.2 A/g.

Fig. 5a shows the CV curves of the porous carbons at the scan rate of 60 mV/s. All the curves present similar symmetric triangular shape and they were a little deviation from ideal rectangular plots. The CV curve enclosed area for C-800 was larger than other materials, which indicated the capacitance of C-800 was higher. Fig. 5b shows the galvanostatic charge/discharge curves of the porous carbons at a current density of 0.2 A/g. The charge/discharge curves exhibited an extremely small deviation from ideal voltage-time curves and similar symmetric triangular shape. There was no obvious voltage drop at the current switches, which suggested that the low resistance of the porous carbon electrode. The

specific capacitances of C-800, C-900 and C-700 obtained at the current density were 221, 212 and 181 F/g, respectively. The porous carbon of C-800 had developed pore structure, and there were a large number of available crosslinked pores. The electrolyte ions could easily shuttled into the carbon materials in the process of charge-discharge, so its specific capacitance was higher than other porous carbons. Compared with the electrochemical performance of other similar materials (189 and 204 F/g at the current density of 0.5 A/g respectively [28, 29], 202.7 and 200 F/g at the current density of 1 A/g respectively [30, 31]), the porous carbon prepared in this work was better. Such excellent electrochemical performance illustrated they had more accessible surface area for the formation of electric double layer and they were expected to be promising electrode materials.

The specific capacitance of porous carbons was influenced by cycle numbers, so the cycling performance of the samples was studied. Fig. 6 shows the change of specific capacitance of porous carbons when the cycle number changes from 1~5000 at a current density of 0.2 A/g. The porous carbons of C-700, C-800 and C-900 showed good cycle stability and there was nearly no loss for their specific capacitance even after 5000 cycles. Whereas, the cycling stability of C-800 was the best, and its specific capacitance retention was about 96.4 % (213 F/g) of the initial value (221 F/g) after 5000 cycles, which was because there were more available crosslinked pores in the material.

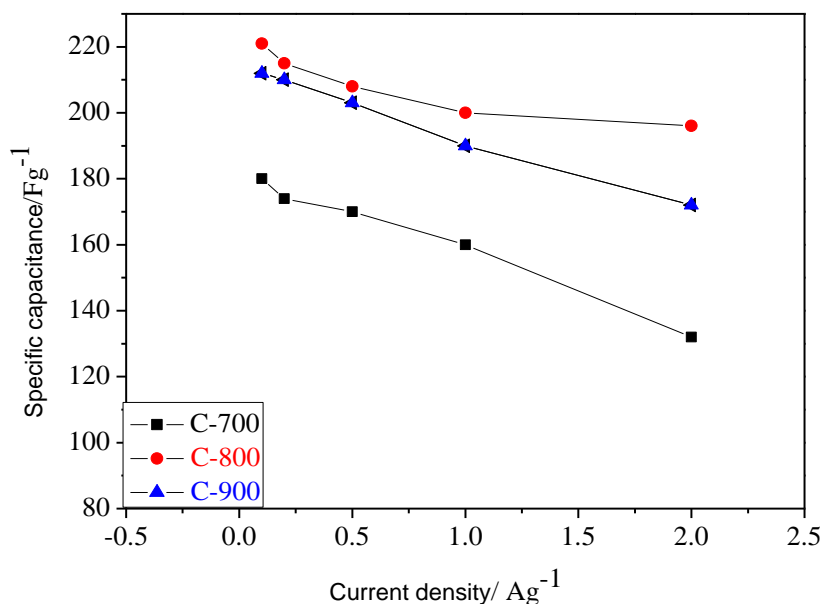


Figure 7. Effect of charge-discharge current density on specific capacitance of the porous carbons.

The relationship between the specific capacitance and the current density was also investigated. Fig. 7 shows the effect of charge-discharge current density on specific capacitance of the porous carbons. Even at a higher current density of 2 A/g, the specific capacitances of C-800, C-900 and C-700 can remain 88.7% (196 F/g), 81.4% (172 F/g) and 73.3% (132 F/g) of the initial value, respectively. At a current density changing from 0.2 to 2 A/g, the C-800 showed higher capacitance retention than other materials.

4. CONCLUSION

In summary, the hierarchical porous carbon material was synthesized by a facile route. The effects of the reaction conditions on pore structure and the electrochemical performance had been studied. The porous carbons presented wide pore size distribution, the pore sizes was mainly distributed at 2 nm (microporous), 9 and 13 nm (mesoporous), which was facilitate to the development of electrochemical performance. In this paper, the capacitance of C-800 was the largest, its maximum specific capacity could achieve 221 F/g, and it demonstrated a superior cyclic stability, which was a promising electrode material for supercapacitors.

ACKNOWLEDGEMENTS

This research was supported by Natural Science Foundation of Tianjin (No. 14JCYBJC17500 and 15JCQNJC05700) and National Students' Platform for Innovation and Entrepreneurship Training Program (No. 201510058020).

References

1. L. Ding, B. Zou, Y. Li, H. Liu, Z. Wang, C. Zhao, Y. Su, Y. Guo, *Mater. Lett.* 74 (2012) 111-114.
2. Ch. Ma, Y. Li, J. Shi, Y. Song, L. Liu, *Chem. Eng. J.* 249 (2014) 216-225.
3. K. Krishnamoorthy, G.K. Veerasubramani, S. Radhakrishnan, S.J. Kim, *Chem. Eng. J.* 251 (2014) 116-122.
4. R.S. Ray, B. Sarma, A.L. Jurovitzki, M. Misra, *Chem. Eng. J.* 260 (2015) 671-683.
5. P. Simon and Y. Gogotsi, *Nat. Mater.* 7 (2008) 845-854.
6. C. Merlet, B. Rotenberg, P.A. Madden, P.L. Taberna, P. Simon, Y. Gogotsi, M. Salanne, *Nat. Mater.* 11 (2012) 306-310.
7. C. Zheng, Y. Qin, D. Weng, Q.F. Xiao, Y. Peng, X. Wang, *Adv. Funct. Mater.* 19 (2009) 3420-3426.
8. N. Li, J. Xu, L. Xu, J. Du, X. Wang, *J. Nanosci. Nanotechno.* 15 (2015) 4961-4968.
9. C. Wang, F. Li, Y. Wang, H. Qu, X. Yi, Y. Lu, *J. Alloy. Compd.* 634 (2015) 12-18.
10. K. Chen and D. Xue, *J. Colloid Interf. Sci.* 446 (2015) 77-83.
11. S. Zhong, C. Zhan, D. Cao, *Carbon* 85 (2015) 51-59.
12. X. Fan, C. Yu, Z. Ling, J. Yang, J. Qiu, *Appl. Mater. Interfaces* 5 (2013) 2104-2110.
13. H.L. Guo, Q.M. Gao, *J. Power Sources* 186 (2009) 551-556.
14. H. Yamada, I. Moriguchi, T. Kudo, *J. Power Sources* 175 (2008) 651-656.
15. K.S. Xia, Q.M. Gao, J. Jiang, J. Hu, *Carbon* 46 (2008) 1718-1726.
16. W. Xing, C.C. Huang, S.P. Zhuo, X. Yuan, G.Q. Wang, D. Hulicova-Jurcakova, Z.F. Yan, *Carbon* 47 (2009) 1715-1722.
17. W. Xing, S.Z. Qiao, R.G. Ding, F. Li, G.Q. Lu, Z.F. Yan, H.M. Cheng, *Carbon* 44 (2006) 216-224.
18. S.C. Wei, D.T. Li, Z. Huang, Y.Q. Huang, F. Wang, *Bioresour. Technol.* 134 (2013) 407-411.
19. Z.X. Ma, T. Kyotani, A. Tomita, *Chem. Commun.* 236 (2000) 2365-2366.
20. Y.K. Kim, K.P. Rajesh, J.S. Yu, *J. Hazard. Mater.* 260 (2013) 350-357.
21. M.J. Valero-Romero, E.M. Márquez-Franco, J. Bedia, J. Rodríguez-Mirasol, T. Cordero, *Micropor. Mesopor. Mater.* 196 (2014) 68-78.
22. Y.X. Kong, T.T. Qiu, J. Qiu, *Appl. Surf. Sci.* 265 (2013) 352-357.
23. D. Liu, W. Yuan, P. Yuan, W. Yu, D. Tan, H. Liu, H. He, *Appl. Surf. Sci.* 282 (2013) 838-843.
24. L.C.A. Oliveira, E. Pereira, I.R. Guimaraes, A. Vallone, M. Pereirac, J.P. Mesquita, K. Sapag, *J. Hazard. Mater.* 165 (2009) 87-94.

25. H. Hadoun, Z. Sadaoui, N. Souami, D. Sahel, I. Toumert, *Appl. Surf. Sci.* 280 (2013) 1-7.
26. Z. Wang, E. Nie, J. Li, Y. Zhao, X. Luo, Z. Zheng, *J. Hazard. Mater.* 188 (2011) 29-36.
27. X. Fan, C. Yu, Z. Ling, J. Yang, J. Qiu, *Appl. Mater. Interfaces* 5 (2013) 2104-2110.
28. Q. Hao, X. Xia, W. Lei, W. Wang, J. Qiu, *Carbon* 81 (2015) 552-563.
29. Y. Wang, B. Chang, D. Guan, X. Dong, *J. Solid State Electrochem.* 19 (2015) 1783-1791.
30. X. Huang, Q. Wang, X.Y. Chen, Z.J. Zhang, *J. Electroanal. Chem.* 748 (2015) 23-33.
31. J. Zeng, Q. Cao, X. Wang, Jing. B, X. Peng, X. Tang, *J. Solid State Electrochem.* 19 (2015) 1591-1597.

© 2016 The Authors. Published by ESG (www.electrochemsci.org). This article is an open access article distributed under the terms and conditions of the Creative Commons Attribution license (<http://creativecommons.org/licenses/by/4.0/>).